

SURVEY OF BALLISTIC LUNAR TRANSFERS TO NEAR RECTILINEAR HALO ORBIT

**Nathan L. Parrish,^{*} Ethan Kayser,[†] Shreya Udupa,[‡] Jeffrey S. Parker,[‡]
Bradley W. Cheetham,[§] and Diane C. Davis^{**}**

This paper presents a survey of ballistic lunar transfer (BLT) trajectories from Earth launch to insertion into a near rectilinear halo orbit (NRHO). Results are described from a detailed set of related mission design studies: the evolution over time of families with and without an outbound lunar flyby; analysis of eclipses; analysis of the ΔV requirements of changing arrival time to rendezvous; and description of the trade space for time of flight vs deterministic ΔV . An ephemeris model is used throughout. These analyses are presented in order to inform future missions to NRHOs.

INTRODUCTION & MOTIVATION

This paper provides a thorough review of how ballistic lunar transfers (BLTs) can be used to transfer from Earth to near rectilinear halo orbits (NRHOs) in an efficient manner. BLTs are a type of low-energy transfer in which a spacecraft launches 1-2 million kilometers away from the Earth (where the Sun's gravity perturbation becomes dominant), then returns to Earth with a larger radius of perigee than before and a different geocentric orbit plane. When designed with the proper geometry, it is possible to choose the perigee to coincide with the Moon's orbit, bringing the spacecraft into the vicinity of the Moon. For many three-body target orbits, it is possible to design the transfer such that it arrives at the target orbit with very little insertion ΔV required. In the ideal case, the transfer is ballistic (zero deterministic ΔV) after launch.¹ This type of transfer is being considered to deliver the Logistics Module, lander elements, and other cargo to the lunar Gateway. Background information on NRHOs is given below. This paper identifies and studies several favorable families of BLTs, where a family is defined as a set of solutions that are topologically distinct from other sets of solutions. Tens of thousands of possible trajectories have been generated, optimized, and evaluated in order to understand the trade space.

In order to quantify the benefits of a BLT compared to a direct lunar transfer in terms of delivered mass, an analysis is performed. The expected performance of the SLS Block 1 launch vehicle² (characterized as maximum launch mass as a function of characteristic energy C3) is used in conjunction with an assumed spacecraft propulsion system Isp of 300 seconds. The resulting mass delivered to NRHO is shown in Figure 1. Proportional benefits exist for other launch vehicles as well.

The benefits of BLTs to an NRHO include: reduced spacecraft ΔV (50-150 m/s depending on the desired launch period, compared to 350-550 m/s for direct transfers), increased mass delivered to the cislunar environment, reduced operational cadence, more launch opportunities, and the ability to send secondary payloads to anywhere in cislunar space. These benefits require trades including: increased time of flight (12 to 20

^{*} Optimization Lead, Advanced Space LLC, 2100 Central Ave, Boulder CO 80301.

[†] Aerospace Engineer, Advanced Space LLC, 2100 Central Ave, Boulder CO 80301.

[‡] Chief Technology Officer, Advanced Space LLC, 2100 Central Ave, Boulder CO 80301.

[§] Chief Executive Officer, Advanced Space LLC, 2100 Central Ave, Boulder CO 80301.

^{**} Principal Systems Engineer, ai solutions, 2224 Bay Area Blvd #415, Houston TX 77058.

weeks, compared to a few days for direct transfers), greater maximum distance from the Earth, increased operations duration, and a higher C3 for some launch options. These benefits and trades are expanded upon in this paper. Further studies will characterize the costs/benefits of navigating BLTs to NRHOs compared to direct transfers.

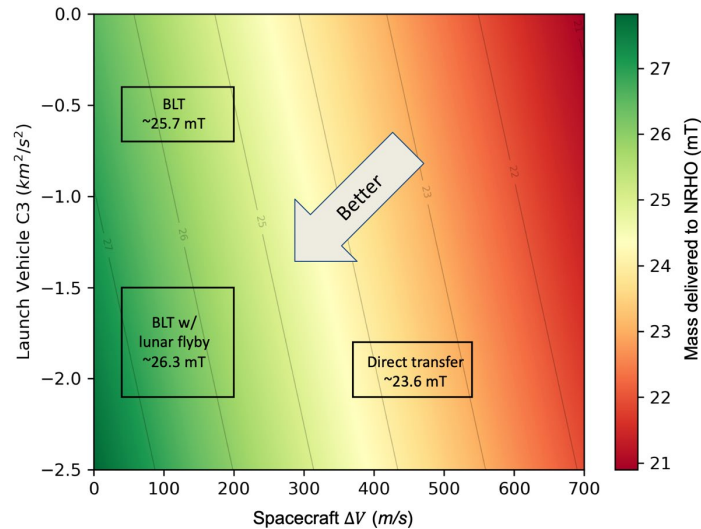


Figure 1. Delivered dry mass for SLS Block 1.

The analysis presented in this paper finds that BLTs are available with wide launch periods. Transfers to the Moon are highly affected by the inclination of the Moon’s orbit relative to an Earth equator frame, which oscillates between approximately 18° and 28° with a period of approximately 18.6 years. BLTs take advantage of the Sun’s gravity to perform an inclination change, thus offering frequent launch opportunities regardless of the Moon’s inclination.

Dynamics and assumptions

Spacecraft dynamics are modeled in the Copernicus trajectory design and optimization system.³ The forces modeled are:

- Sun, Earth, and Moon point masses, with states from the JPL DE430 ephemerides⁴. A spherical harmonics gravity model of the Moon is used for some studies as described below.
- Solar radiation pressure, with a cannonball model and assuming mass of 14,000 kg, surface area of 23 m^2 , and coefficient of reflectivity of 2.0. These are chosen to be representative of the Logistics Module for the Gateway.

Other gravitational bodies and perturbations are not considered. All maneuvers are assumed to be impulsive changes in velocity (ΔV). Launch is not modeled. The simulation begins in a 100 km circular parking orbit around Earth with inclination of 28.5° , approximating the condition immediately after launch from Kennedy Space Center.

The initial analysis of BLTs in this study uses a point mass model of the Moon. After the initial analysis, more fidelity is added: spherical harmonics with degree and order 8 using the GRGM660PRIM gravity model, derived from GRAIL. Due to the sensitivity of the dynamics in the NRHO, switching to the more accurate force model is found to noticeably impact the direction of the insertion maneuver.

Another simplifying assumption used for part of the analysis is to target an NRHO with the correct period, but which is not fixed in time. NRHOs are only truly periodic in the circular restricted three body problem (CRTBP) dynamics; when an ephemeris model is used, they become quasi-periodic. There is a set of equally-valid NRHOs for any given orbital “period”. The initial analysis uses an NRHO defined by convenience, which allows the optimization algorithm to place perilune at any epoch. These transfers are referred to as “phase-free”. Subsequent analysis on some transfer options explores “phase-fixed” transfers, in which the

final state is constrained to rendezvous with a particular reference NRHO. The phase-fixed transfers are more applicable to real operations and impose more restrictive constraints on the problem.

BACKGROUND

Near Rectilinear Halo Orbits

NRHOs represent a subset of the L1 and L2 halo orbits, bounded by changes in linear stability.⁵⁻⁹ Their name comes from the fact that they appear to have eccentricity of nearly 1.0 relative to the Moon when viewed in a Moon-centered, Earth-Moon rotating frame. For some NRHO orbit periods, the dynamics are linearly stable (in the Earth-Moon circular restricted three-body dynamics), and for others, the dynamics are linearly unstable. The current nominal orbit for the Gateway is a 9:2 synodic-resonant southern L2 NRHO, meaning that the spacecraft completes 9 revolutions about the Moon for every 2 synodic revolutions of the Moon about the Earth. This resonance is favorable because it minimizes the amount of time spent in the Earth's shadow. NRHOs with a 9:2 resonance are slightly linearly unstable. When simulated with high-fidelity dynamics, all NRHOs are slightly unstable. Results from the literature have found that small maneuvers can maintain a safe orbit for a ΔV cost on the order of a few meters per second per year.^{8,10}

Ballistic Lunar Transfers

A truly ballistic lunar transfer trajectory is one which (with a perfect launch) requires no propulsion between launch and orbit insertion. Such a transfer is made possible by leveraging the gravitational attraction of Earth, Sun, and Moon. An example trajectory is plotted in the inertial J2000 reference frame in Figure 2.

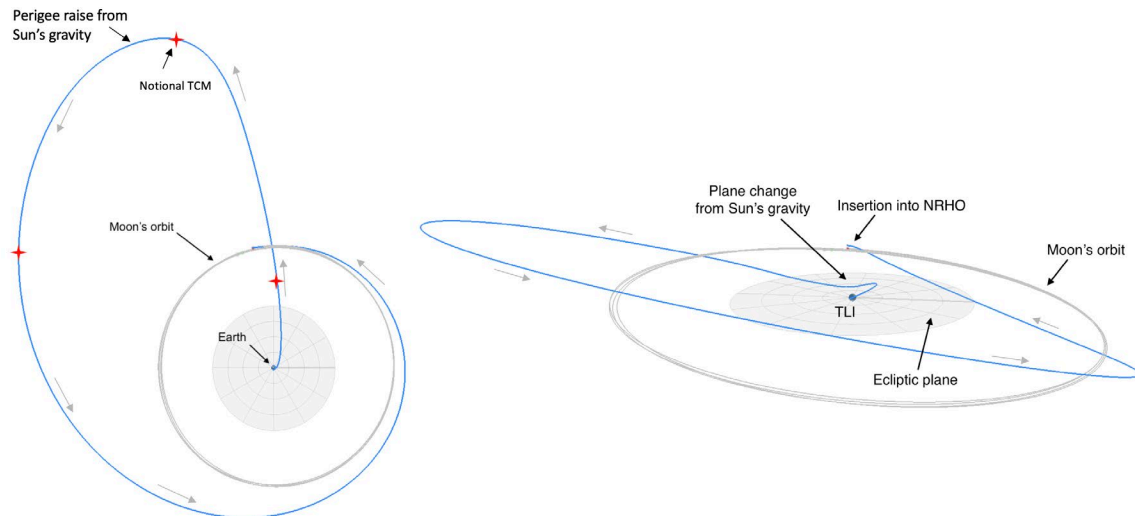


Figure 2. A BLT viewed in an inertial frame, top-down and inclined views.

In practice, ballistic trajectories only exist at a limited number of instantaneous launch opportunities when the geometry of the Sun-Earth-Moon system aligns perfectly. In addition to the notional trajectory correction maneuvers (TCMs) shown in the figure, deep space maneuvers (DSMs) on the order of tens of meters per second open up daily launch opportunities by patching together the set of achievable launch states and the set of achievable NRHO insertion states.

The transfers studied here use a deterministic NRHO insertion maneuver as well as one or more deterministic DSMs. If all the maneuvers are executed perfectly, the deterministic ΔV represents the full fuel cost. In practice, periodic trajectory correction maneuvers are also required to account for uncertainties such as injection errors, maneuver execution errors, and navigation uncertainty. These statistical maneuvers are not considered in this analysis.

The Sun's gravity has a coupled effect on the perigee and the orbit plane with respect to Earth. As a result of this coupling, transfers vary at monthly and yearly frequencies. Monthly variations are driven by the

Moon's motion about its orbit and the Moon's orbit eccentricity, and yearly variations are driven by the approximately 5.1° offset between the Moon's orbit plane and the ecliptic plane and the approximately 28° offset between the Earth's polar axis and the ecliptic plane. The geometry of BLTs is constrained by several factors, including: latitude of the launch site, direction of apogee relative to Sun and Earth, and rendezvous with the target NRHO at the Moon.

The transfer can be considered in multiple parts, depending on which gravitational body is driving the motion. The first segment is launch and the trans-lunar injection (TLI) burn, which sends the spacecraft to an apogee in the range of 1-2 million kilometers, or 3-5 times the distance from Earth to Moon. The second segment is defined near apogee. When the apogee is in the second or fourth quadrant of an Earth-centered, Sun-Earth rotating frame, the Sun's gravity raises radius of perigee (r_p) from a few hundred kilometers up to the altitude of the Moon's orbit, and it reduces inclination relative to Earth. BLTs take advantage of this effect to raise perigee from the parking orbit altitude up to the radius of the Moon's orbit. Figure 3 illustrates transfers viewed in an Earth-centered, Sun-Earth rotating frame. The four quadrants are defined, and the effects of solar gravity are marked in red arrows. These effects apply to a trajectory with apogee located in the specified quadrant.

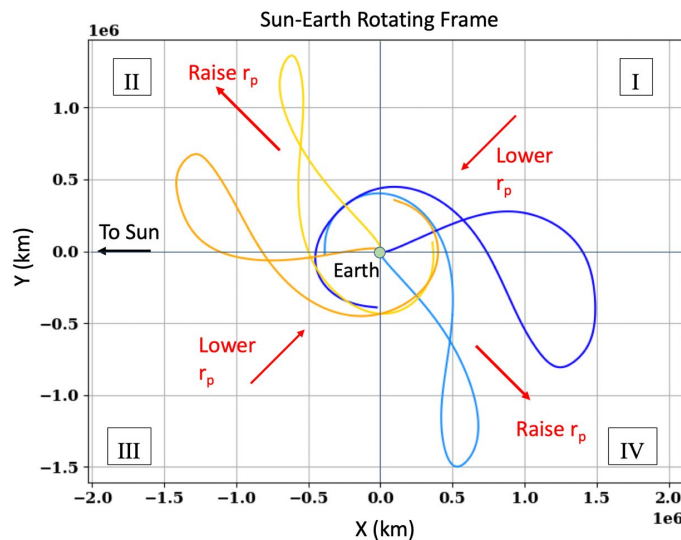


Figure 3. BLT families without a lunar flyby, in Sun-Earth rotating frame.

The third and final phase of a BLT is when it comes in to the newly raised perigee and enters the vicinity of the Moon. Transfers exist that arrive in the vicinity of the Moon with a low orbital energy relative to the Moon. When the target orbit is unstable (such as a halo orbit near the L_1 or L_2 libration points orbits), the arriving trajectory near the Moon can be designed to lie on the stable manifold of the libration point orbit. In principle, the spacecraft can “insert” into the NRHO for an infinitesimally small ΔV . In practice, such an arrival strategy involves many revolutions winding on the NRHO, and the time of flight is untenable. There is a direct correlation between the time of flight and the deterministic insertion ΔV , analyzed in this paper.

RESULTS

Ballistic lunar transfers are presented here as members of 16 unique families (topologically distinct groups of solutions). Transfers without a lunar flyby are presented first, followed by transfers with a lunar flyby on the outbound trajectory. Each group of families of solutions is studied as “phase-free” and “phase-fixed”. In both cases, the insertion maneuver is nominally performed at perilune. For the phase-free transfers, the epoch of the perilune insertion is a free parameter that can be optimized. For the phase-fixed transfers, the epoch of the perilune insertion must match one of the perilune epochs from a Gateway reference orbit defined by a SPICE kernel file. Following the insertion maneuver at perilune, one or more subsequent maneuvers are performed to rendezvous with the reference orbit. A preliminary rendezvous analysis is presented consisting of one additional rendezvous maneuver with favorable characteristics.

Families of BLTs

In the literature, studies of BLTs in the Sun-Earth CRTBP have found many families of solutions that do not have a lunar flyby, and even more families of solutions that do have a lunar flyby.^{1,11} Some of these families exist so close to each other that they are equivalent in terms of practical implementation. In the current study, an ephemeris model is used, which enforces stricter geometry constraints than the time-independent CRTBP. As a result, the four families (without a lunar flyby) in Reference ¹² clearly become just two families, and two more are added based on whether the trans-lunar injection (TLI) maneuver is performed near the ascending node or the descending node of the parking orbit. When lunar flyby trajectories are considered, more families become apparent. The BLTs with a lunar flyby are differentiated by three key parameters: TLI performed near the ascending node or descending node, apogee in quadrant II or IV of the Sun-Earth rotating frame (or, more colloquially, apogee “towards” the Sun or “away” from the Sun), and the length of time between the initial flyby and insertion into the NRHO (“short”, “medium”, or “long”). Considering all combinations of these parameters yields 12 additional families. A list of the families considered here is given in Table 1.

Table 1. List of families of BLTs.

#	TLI approx. location	Apogee quadrant	Lunar flyby	# of Moon orbits between flyby & insertion
1	Ascending node	II (towards Sun)	No	N/A
2	Descending node	II (towards Sun)	No	N/A
3	Ascending node	IV (away from Sun)	No	N/A
4	Descending node	IV (away from Sun)	No	N/A
5	Ascending node	II (towards Sun)	Yes	4
6	Ascending node	II (towards Sun)	Yes	5
7	Ascending node	II (towards Sun)	Yes	5-6
8	Ascending node	IV (away from Sun)	Yes	4
9	Ascending node	IV (away from Sun)	Yes	5
10	Ascending node	IV (away from Sun)	Yes	5-6
11	Descending node	II (towards Sun)	Yes	4
12	Descending node	II (towards Sun)	Yes	5
13	Descending node	II (towards Sun)	Yes	5-6
14	Descending node	IV (away from Sun)	Yes	4
15	Descending node	IV (away from Sun)	Yes	5
16	Descending node	IV (away from Sun)	Yes	5-6

Thus, a total of 16 topologically distinct families of BLTs are identified in this study. Each family is classified according to a few defining geometry constraints. Additional families exist beyond this list. Each of these “families” also contains “sub-families” that are not classified in the current study. A representative subset is studied in detail. It is found that the true anomaly of the TLI maneuver (which determines whether TLI is near the ascending or descending node) is best driven by the optimization algorithm. For any given family on any given epoch, both ascending node and descending node solutions exist. Typically, one requires significantly less ΔV than the other, so it is not necessary to study all combinations in detail.

Phase-Free BLTs without Lunar Flyby

The evolution of the first four families (no lunar flyby) is examined in Figure 4 and Figure 5. In these figures, Earth departure epoch is the independent variable. The following parameters are optimized using a continuation method from the adjacent Earth departure epochs: parking orbit right ascension of the ascending node (RAAN), true anomaly at TLI, a single deep space maneuver (DSM), NRHO insertion epoch, and the NRHO insertion maneuver. The optimization objective is to minimize the total post-TLI ΔV .

These figures show the variation of key parameters as a function of Earth departure epoch. The monthly repeating patterns are clearly apparent for total spacecraft ΔV , launch vehicle C3, and transfer duration. Note that these transfers arrive in a “phase-independent” NRHO, meaning the NRHO perilune can occur at any epoch. When the insertion maneuver is constrained to lie on a particular reference NRHO, the ΔV cost generally increases. Rendezvous is studied further in a later section.

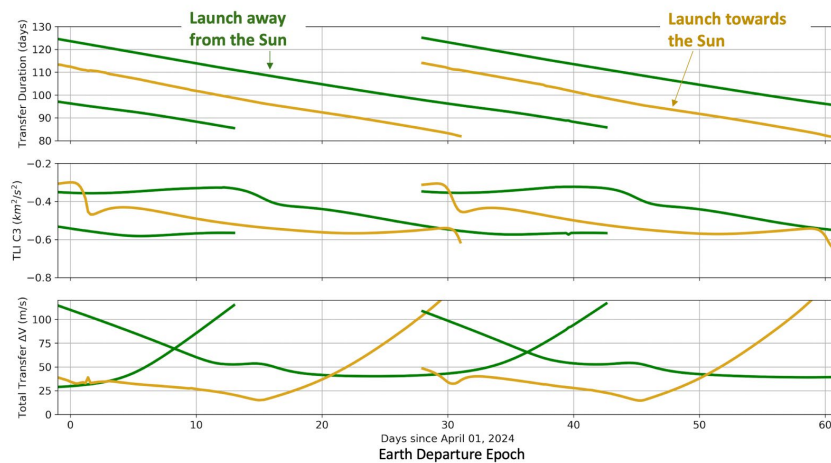


Figure 4. Evolution of families with TLI near descending node.

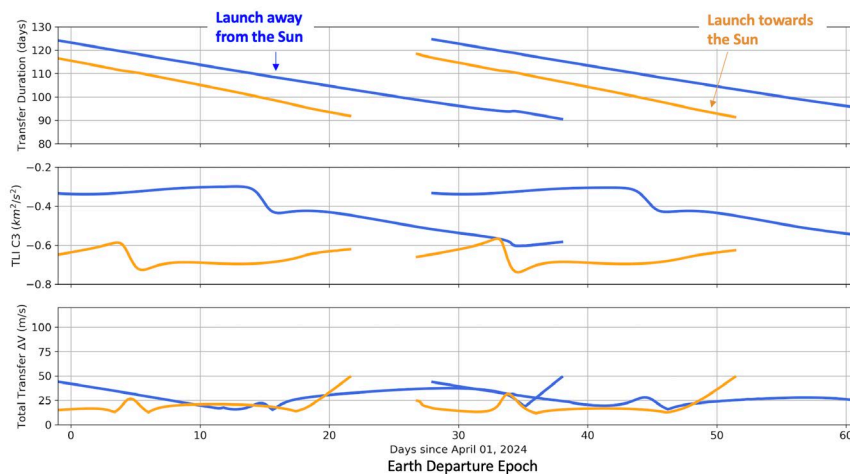


Figure 5. Evolution of families with TLI near ascending node.

It is natural to visualize BLTs in the Sun-Earth rotating frame, where the x-axis points from Sun to Earth, the z-axis is aligned with the system angular momentum vector, and the y-axis completes the right-handed coordinate frame. Figure 6 and Figure 7 each show a single month's solutions for one family. Note that in all cases, the direction of apogee is carefully targeted such that perigee is raised to the radius of the Moon's orbit and the geocentric orbit plane is aligned with a state approximating the NRHO stable manifold. Flexibility in the NRHO insertion epoch gives an extra degree of freedom to align the orbit planes. When this degree of freedom is later removed in order to enforce rendezvous with a reference, the ΔV costs rise.

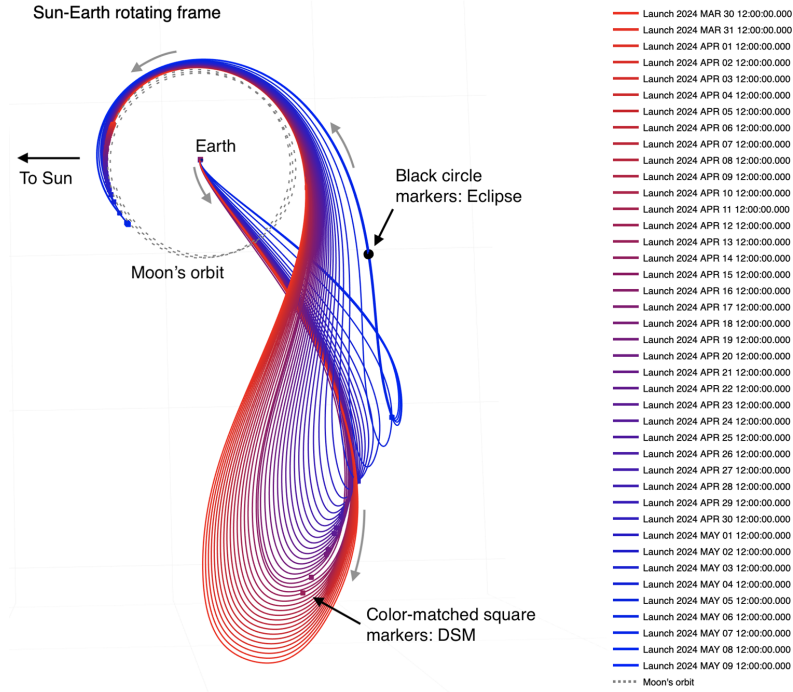


Figure 6. Daily solutions for one month from the family "ascending, away", viewed in the Sun-Earth rotating frame. Black circles denote eclipses, which only occur during the end of the month.

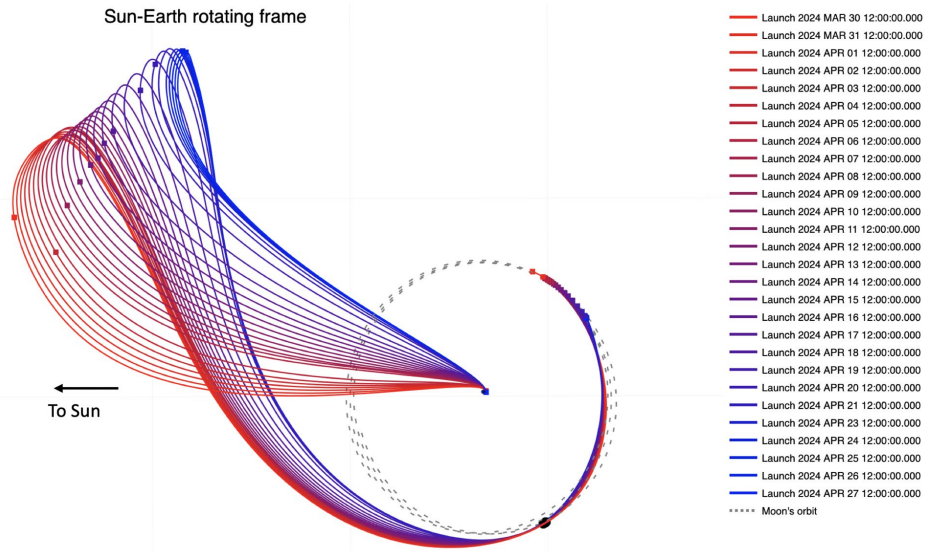


Figure 7. Daily solutions for one month from the family "ascending, towards", viewed in the Sun-Earth rotating frame. Black circles denote eclipses, which only occur during the end of the month.

Eclipse durations are also considered in this study. It is found that, for any given family of transfers, there are some Earth departure epochs at which the spacecraft passes through the Moon's shadow for on the order of a few hours. In a given month, there are typically 1-3 launch dates that have eclipses of up to 3 hours. Short Earth eclipses (<10 minutes) exist for most TLI epochs and occur immediately after TLI. Higher-fidelity simulation of the launch conditions is required to describe the Earth shadowing accurately. If it is necessary to avoid eclipses, switching to a different family of transfers for part of the month is an effective mitigation, as each family has eclipses at different TLI epochs.

Phase-Free BLTs with Lunar Flyby

Several additional families of trajectories exist that use a lunar flyby on the outbound trajectory. The lunar flyby adds energy to the spacecraft that would otherwise have to come from the launch vehicle, so the launch C3 requirement is reduced from approximately $-0.7 \text{ km}^2/\text{s}^2$ to approximately $-2 \text{ km}^2/\text{s}^2$, similar to the C3 required for a direct transfer to an NRHO.

A set of six families of solutions is found that have low ΔV and provide a range of feasible options. The families are mostly characterized by time of flight ("short" transfers of approximately 110-130 days, "medium" transfers of approximately 140-160 days, and "long" transfers of approximately 160-180 days) and by the apogee direction in the Sun-Earth rotating frame (either "towards" the Sun or "away" from the Sun). Six families are shown in Figure 8.

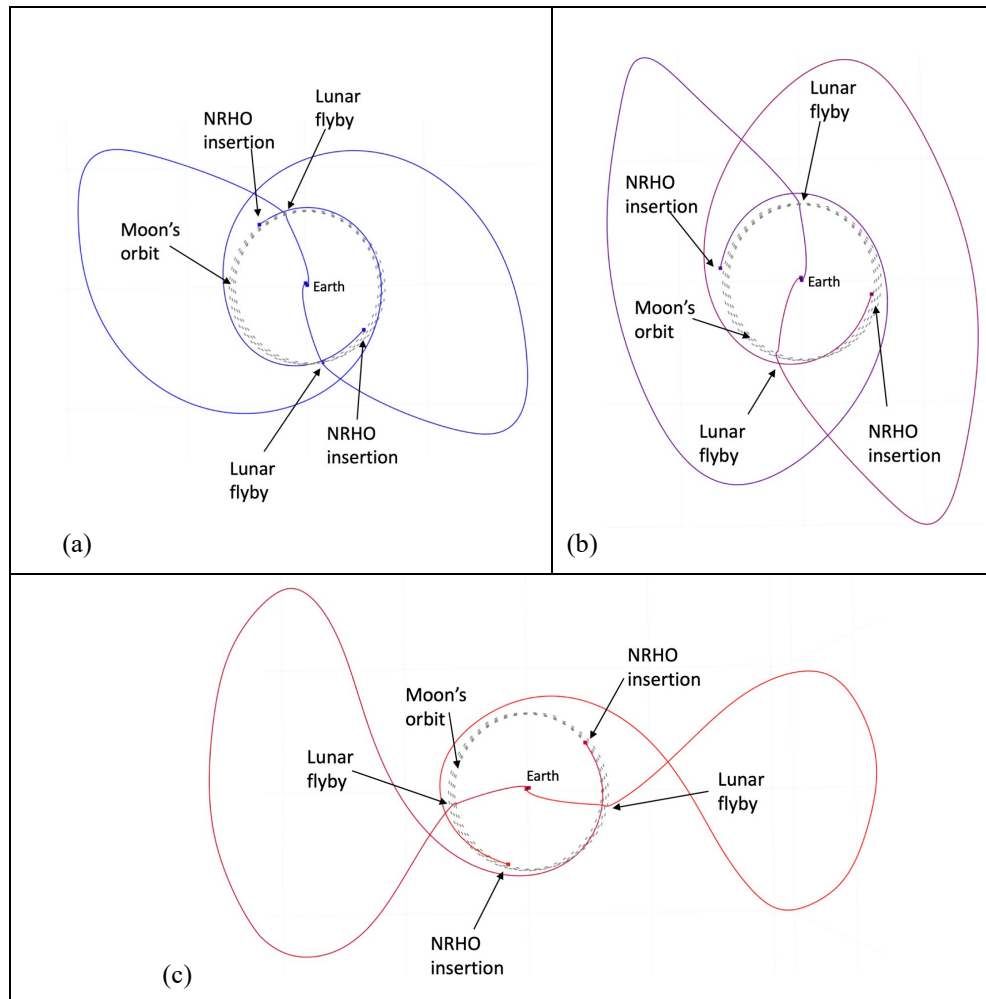


Figure 8. Short (a), medium (b), and long (c) families of BLTs with lunar flyby. Shown in the Sun-Earth rotating frame, with the Sun far to the left.

Other trajectory options also exist, but the families in Figure 8 have lower spacecraft ΔV , lower launch vehicle C3, and occur every month over a year. The less favorable solutions are not included. It is notable that the “towards” and “away” versions of each family are closely approximated by a 180° rotation about the z-axis of the rotating frame (the angular momentum vector of the Sun-Earth system).

Another important characteristic of this set of families is that each family optimally flies by the Moon at a different epoch. This trait opens up the launch period. For any BLT that performs a flyby of the Moon on the outbound leg, the flyby occurs approximately 2-4 days after TLI. The location of the lunar flyby in the Sun-Earth rotating frame is a major driver of the whole transfer. By jumping from family to family, the set of acceptable TLI epochs grows.

Locally optimal solutions with a lunar flyby are found by minimizing a weighted combination of ΔV from TLI, deep space maneuvers, and NRHO insertion. The main benefit of BLT-type trajectories is that the ΔV performed by the spacecraft is minimized, so intuition suggests that the TLI ΔV should not be considered in the objective function. However, the main goal of the outbound lunar flyby is to reduce the launch vehicle C3 requirement. Including the TLI maneuver in the objective function ensures that both launch vehicle C3 and spacecraft ΔV are minimized. Future studies with known launch vehicle performance can constrain TLI to the launch vehicle’s specifications and focus on delivered payload instead.

Studies are performed to understand the robustness of each of these families of transfers with regard to Earth departure date (which determines launch period) and NRHO arrival date (which determines the cost of rendezvous with a particular reference NRHO). As an example, the evolution of the “short, towards” family of solutions with a lunar flyby is evaluated here as a function of Earth departure epoch. Earth departure epoch is varied by ± 5 days, and NRHO arrival epoch is a free parameter chosen to minimize the weighted sum of spacecraft ΔV and launch vehicle C3. A continuation method is used, where the Earth departure epoch is gradually increased or decreased. Each converged solution is used to initialize the next Earth departure epoch.

Figure 9 shows this set of trajectories overlaid together in the Sun-Earth rotating frame. The beginning of the launch period is shown in red, and the close of the launch period in blue. Figure 10 shows the evolution of key parameters for this same set of transfers.

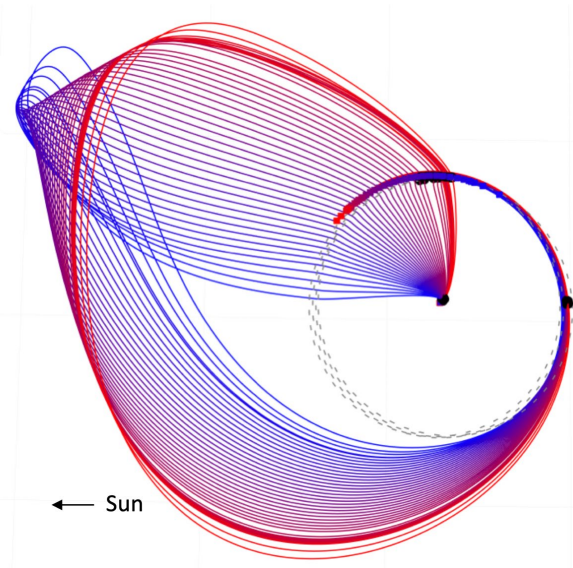


Figure 9. Solutions of the “short, towards” lunar flyby family over one launch period. Viewed in the Sun-Earth rotating frame.

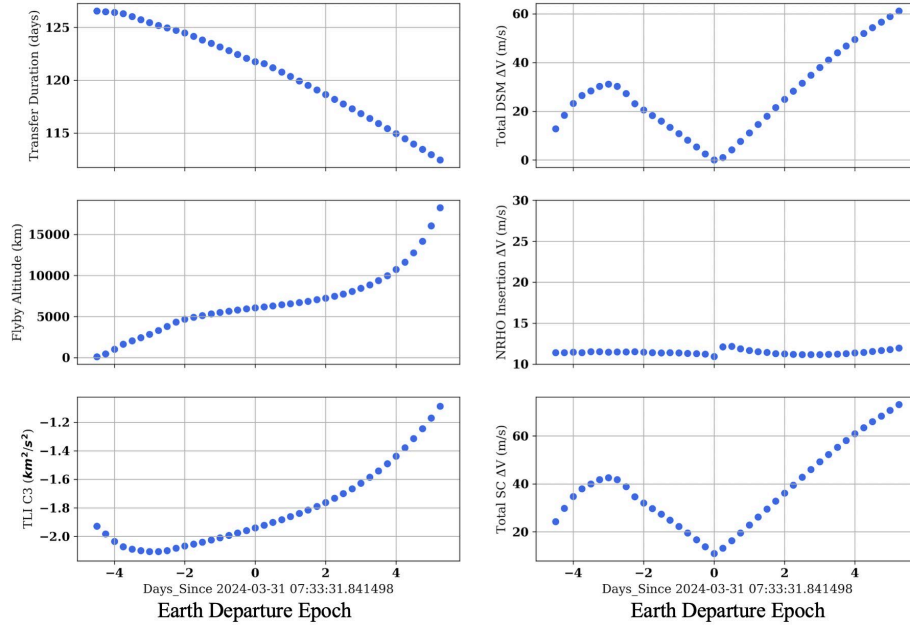


Figure 10. Evolution of “short, towards, LFB” family over one launch period.

The “short, towards” family is then evaluated for each synodic month of a year, using continuation to jump from month to month. The epochs of TLI, deep space maneuver(s), and NRHO insertion are all increased by 29.5 days (approximately one synodic month). With some small adjustments, a very similar transfer is again found for each month. The month-to-month variation over the course of a year is shown in Figure 11. Annual cyclical trends are apparent in each of the main resulting characteristics: transfer duration, lunar flyby altitude, launch C3, and insertion maneuver magnitude.

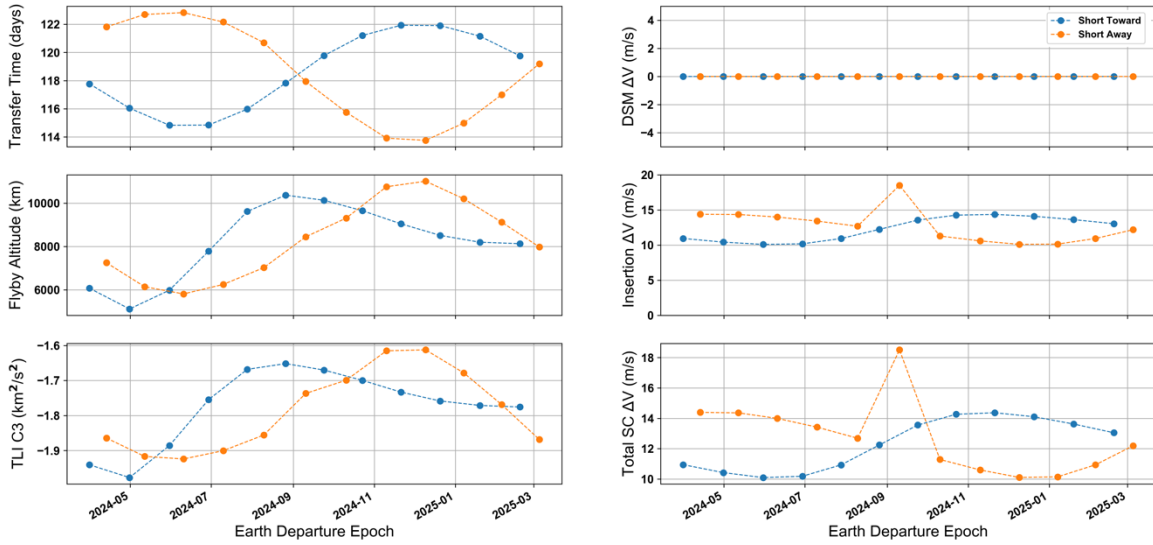


Figure 11. Evolution of “short, towards, LFB” family over one year.

The same analysis is repeated for each of the other five families. For the sake of page length, only partial results are included here. Additional results are in the additional online material available at the link below.*

* <https://advancedspace.com/blt/>

Phase-Fixed BLTs without Lunar Flyby

This section presents results of multiple related studies to understand how to rendezvous with a reference NRHO. This additional phasing constraint is necessary for vehicles headed to the Gateway. The parameters explored are: where in the NRHO (osculating true anomaly) the insertion maneuver should be performed, time spent winding on to the NRHO, the ΔV cost of forcing the BLT to synchronize with a reference NRHO and the resulting launch periods, and how to divide the insertion and rendezvous into multiple maneuvers for safe and efficient operations.

Several options are considered for how to efficiently, practically, and safely rendezvous with the Gateway. The main trade to consider is how much time should be spent winding on to the target NRHO. To first order, the more revolutions of wind-on, the lower the deterministic ΔV and the higher the time of flight. The analysis in this section assumes rendezvous with a given reference NRHO, increasing the ΔV compared to earlier analysis. Several principles must be simultaneously considered when deciding the NRHO insertion strategy:

- Reducing the time of flight is generally good.
- Reducing the deterministic ΔV is generally good, as is reducing the statistical ΔV . However, these are competing goals in this case.
- At perilune, change in spacecraft kinetic energy is most efficient (lowest ΔV). This is referred to as the Oberth effect.¹³ If the insertion maneuver is performed at perilune, the deterministic ΔV is minimized, but maneuver execution errors are also magnified. Performing the maneuver farther from perilune increases deterministic ΔV but reduces the effect of the maneuver execution errors.
- Collision risk with existing Gateway elements must be mitigated.
- Gradual “wind-on” transfers also have a gradual “wind off” in case the insertion maneuver is not performed. Longer arrivals may be more resilient to missed maneuvers.
- Every perilune passage has a chaotic, multiplicative effect on the spacecraft uncertainty. So, shorter arrivals may be favorable for the predictability of future motion.

Clearly, there are multiple reasons for and against either a short or a long insertion wind-on. For this study, insertion conditions with 0, 1, and 2 revolutions are considered. An example of each of these wind-on arrival options is given in Figure 12. Further analysis is required to decide which is best for a given mission design.

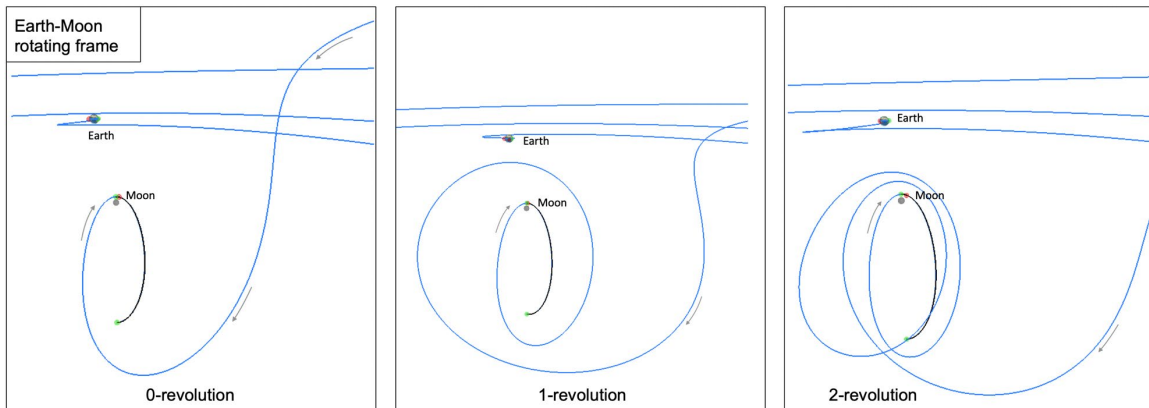


Figure 12. Comparison of NRHO wind-on arrival options.

The first step taken to understand the impact of insertion maneuver timing is to perform the maneuver at perilune, 6 hours after perilune, 12 hours after perilune, and 24 hours after perilune. Figure 13 shows the insertion ΔV and total ΔV (insertion + DSM) for a case where insertion is performed nominally 1 revolution after arriving in the vicinity of the Moon. As expected, the ΔV increases with distance from perilune. The insertion maneuver is approximately in the anti-velocity direction.

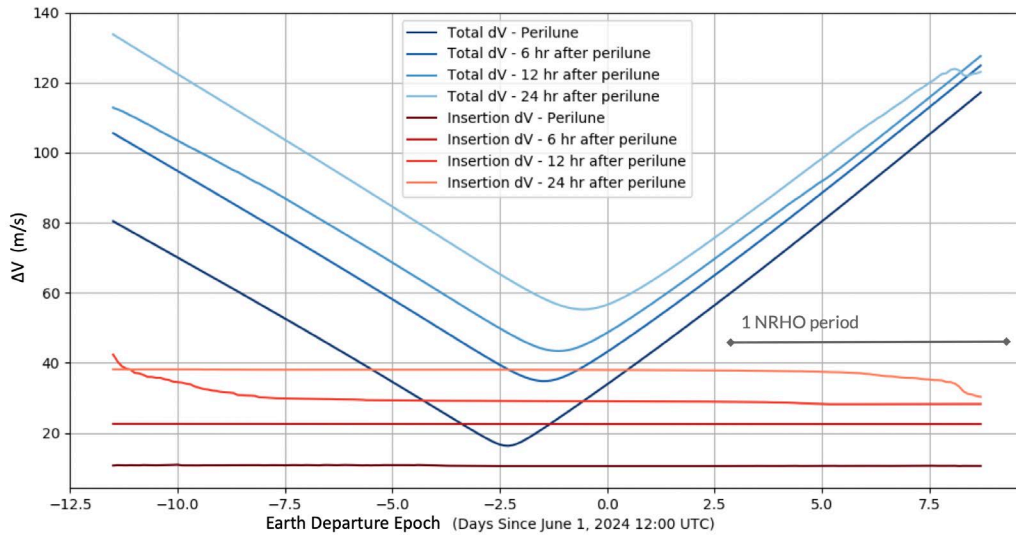


Figure 13. Phase-fixed insertion ΔV as a function of Earth departure epoch, one-revolution wind-on.

It can be more intuitive to think of the arrival backwards in time, which is typically how stable manifolds are generated. When run backwards, the osculating true anomaly of the insertion maneuver determines the direction in which the spacecraft departs the NRHO. Once the spacecraft has left the sphere of influence of the Moon, its motion is dominated by the Earth's gravity. The true anomaly of the insertion maneuver directly drives the geocentric orbit plane. In order to minimize the DSM ΔV , the geocentric orbit plane as the spacecraft approaches NRHO insertion must match the orbit plane after the Sun's gravity perturbation has its effect. Thus, allowing the true anomaly of the insertion maneuver to vary is important for reducing the DSM ΔV .

Davis et. al¹⁴ performed detailed studies of departure from an NRHO. When the dynamics are described in an Earth-Moon rotating frame, motion in the vicinity of a halo orbit is similar forwards and backwards in time. Thus, the departure conditions can give intuitive understanding to the arrival conditions. The departure study suggests the following key points for arrival into an NRHO:

- If the insertion maneuver is performed at perilune, the maneuver should be nominally in the anti-velocity direction.
- If the insertion maneuver is performed at apolune, the maneuver should nominally be in the anti-normal (approximately towards Earth) direction.
- A 5-10 m/s anti-velocity burn at perilune can capture with three revolutions of wind-on.
- A 15 m/s anti-velocity burn at perilune can capture with one revolution of wind-on.
- A 15 m/s anti-normal (approximately towards Earth) maneuver at apolune can capture with three revolutions of wind-on.

These findings, drawn intuitively from the departure analysis, have been found to agree closely with high-fidelity simulations of NRHO insertion. In particular, an “insert then rendezvous” strategy is developed in which the majority of the insertion maneuver is executed at perilune (minimizing deterministic ΔV), and a 1 m/s maneuver is executed at the next apolune (3.3 days later). The apolune rendezvous maneuver is nominally performed in the “orbit normal” direction, where “orbit normal” is defined as the cross product of the Moon-centered position and velocity of the spacecraft in an Earth-Moon rotating frame.

Each 1 m/s of deterministic ΔV allocated for the rendezvous maneuver is found to correspond to approximately 1,100 km in-track separation at perilune between the arriving spacecraft and the existing Gateway elements when the insertion maneuver is performed. Figure 14 shows a view where a 3 m/s maneuver is performed at apolune, resulting in 3,500 km separation between the vehicles when the perilune maneuver is performed. Because the difference in orbital motion at perilune is nearly entirely in the in-track direction, adding the apolune maneuver does not have any significant effect on TLI, DSMs, or perilune insertion

maneuvers. Thus, the arrival analysis can be largely decoupled from the rest of the transfer. A known concern with the arrival strategy as implemented here is that the arriving spacecraft is on a trajectory that will intersect the Gateway rendezvous sphere. Operationally, it will be desirable that visiting spacecraft arrive on a safe, free-drift trajectory that will not intersect the Gateway. Further refinements to the strategy could bias the perilune insertion maneuver to reduce the likelihood of impact, then add one or more maneuvers to rendezvous near apolune.

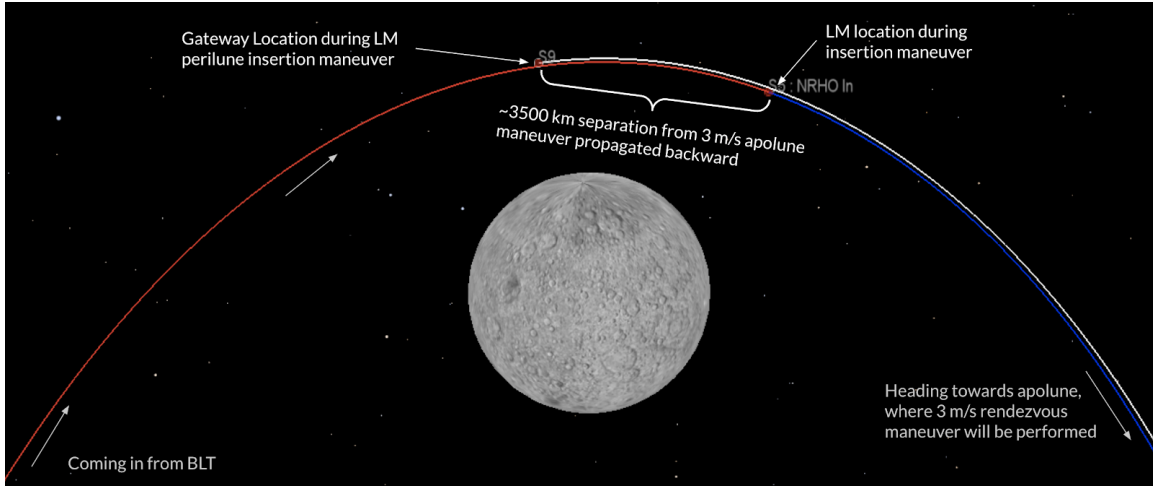


Figure 14. Diagram description of the insert-then-rendezvous (ITR) strategy, designed around a notional Logistics Module (LM) rendezvousing with the Gateway.

This “insert-then-rendezvous (ITR)” strategy is found to be an effective way to maximize the efficiency of the insertion maneuver (at perilune), maintain a safe distance from the Gateway during that insertion maneuver, and perform rendezvous at apolune when relative motion is greatly reduced.

In principle, a “direct” insertion (single maneuver near perilune) or the ITR strategy can be performed after any number of wind-on orbits. The following analysis considers 0-rev, 1-rev, and 2-rev wind-on, each with or without the additional maneuver at apolune. Figure 15 shows the total deterministic spacecraft ΔV for all six cases. Some interesting observations can be made: the direct insertion and ITR strategies are equivalent in ΔV ; and choosing a different number of wind-on orbits based on the Earth departure epoch expands the launch period, in this case by approximately 4 days.

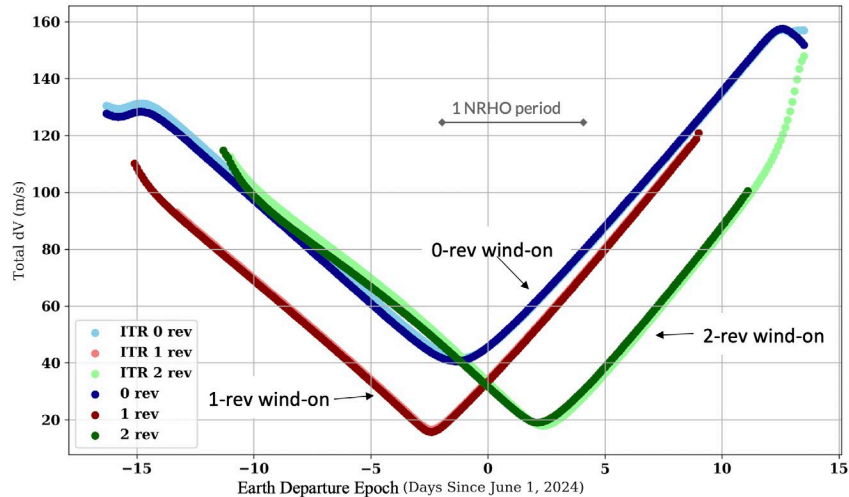


Figure 15. Total ΔV as a function of TLI epoch for an example reference transfer, for various insertion strategies.

The current analysis suggests that nearly all BLTs can be designed such that the deterministic insertion ΔV is under 20 m/s. Most of the variation in ΔV as a function of departure epoch is caused by differences in the DSM. Figure 16 shows the deterministic insertion ΔV to rendezvous with a fixed reference orbit, as a function of Earth departure epoch. The zero-rev wind-on case is constant at approximately 16 m/s across all launch epochs. Adding one revolution of wind-on reduces the deterministic ΔV by 3-5 m/s, and adding a second revolution of wind-on reduces the deterministic ΔV by another 3-5 m/s. Interestingly, the maxima of insertion ΔV correspond to the minima of total ΔV . The ITR strategy changes the insertion ΔV by up to approximately ± 1 m/s in most cases, where the exact amount depends on the launch epoch. Note that these ΔV computations do not include proximity operations and docking costs.

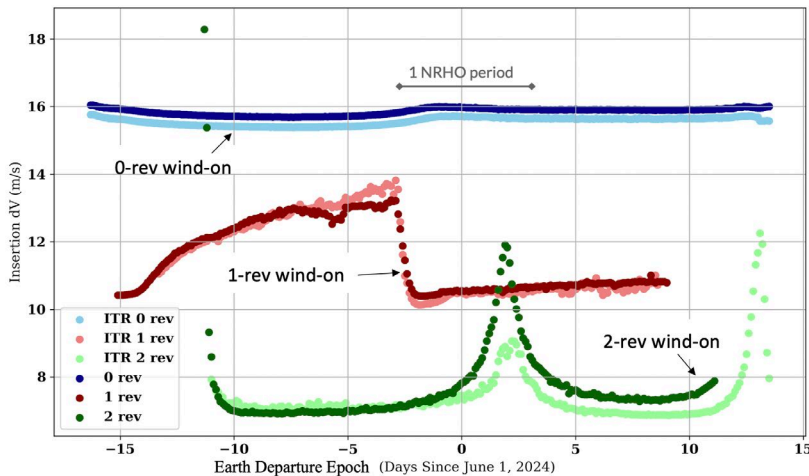


Figure 16. Insertion ΔV as a function of TLI epoch for an example reference transfer, for various insertion strategies.

It is clear from Figures 14-16 that the “direct” and the “ITR” strategies are effectively equivalent in terms of ΔV , while the ITR strategy may be preferable for operational reasons. With this in mind, the zero-revolution ITR strategy is then used to consider a large trade space of departure and arrival epochs. Figure 17 shows deterministic spacecraft ΔV as a function of Earth departure epoch and NRHO arrival epoch. This analysis is similar to the “porkchop” plots often used in early interplanetary mission design. In this figure, two distinct families are captured: those which launch towards the Sun (Quadrant II in the Sun-Earth rotating frame) and those which launch away from the Sun (Quadrant IV in the Sun-Earth rotating frame). The two families are offset in arrival epoch by approximately half of a lunar synodic month. Two additional families exist in the data shown but are not clearly apparent: transfers with the TLI maneuver near the ascending node or the descending node of the parking orbit. In generating the transfers captured here, the osculating true anomaly of TLI is a free optimization parameter.

The black horizontal lines in Figure 17 represent the arrival epochs corresponding to rendezvous with the reference Gateway orbit. Some rendezvous opportunities lie in the green regions of the heat map, representing favorable arrival opportunities for this BLT family. Other arrival epochs, on the other hand, exist in red regions of the heat map, signifying expensive opportunities. In particular, two launch periods within this time frame offer deterministic spacecraft ΔV under 100 m/s. The first launch period is from 2024-04-01 to 2024-04-16, arriving on 2024-07-26. The second launch period is from 2024-04-22 to 2024-05-01, arriving two weeks later on 2024-08-08.

The same analysis is repeated for the months of May and June 2024. The resulting heatmap for June 2024 appears in Figure 18. Note that for this month, distant lunar flybys are captured in the design results for part of the analysis period. It is possible to design solutions without lunar flyby in these parts of the solution space, but the authors decided to keep these features in the data to illustrate how multiple families can overlap with each other. The figure also shows several “pixels” that do not match the smooth pattern around them. These are similarly caused by the optimization approach finding slightly different “sub-families” of solutions that exist adjacent to each other in the state space.

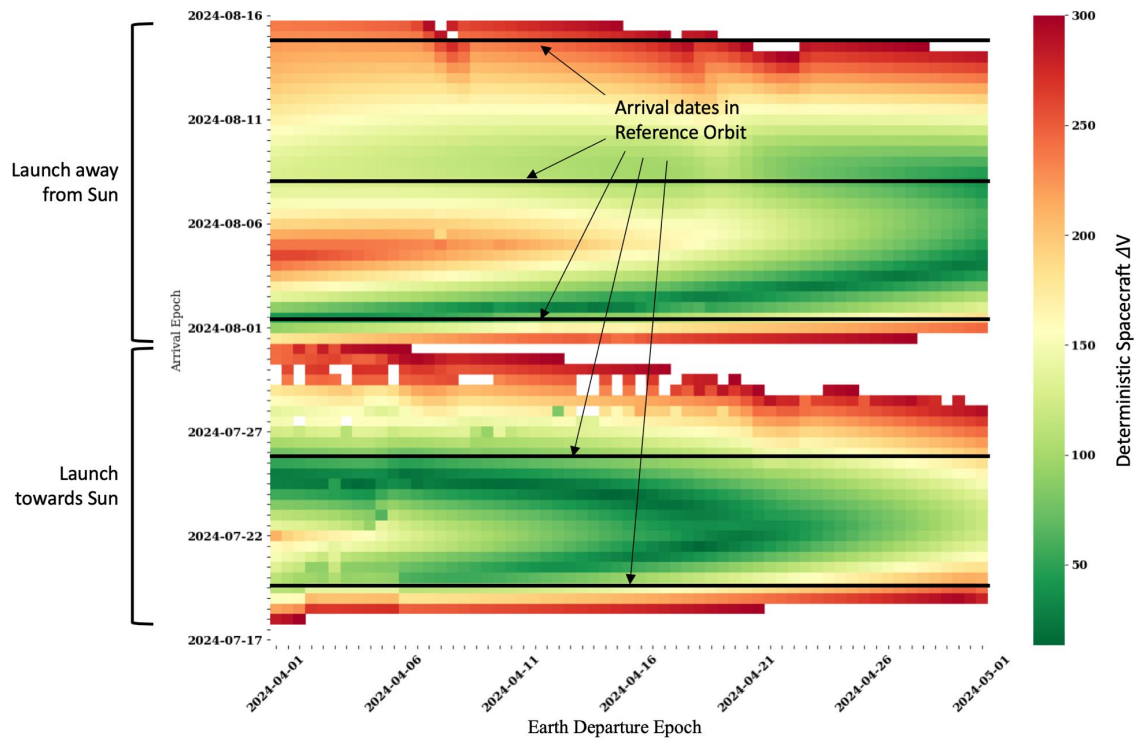


Figure 17. Heatmap of deterministic spacecraft ΔV as a function of Earth departure epoch and NRHO arrival epoch, April 2024.

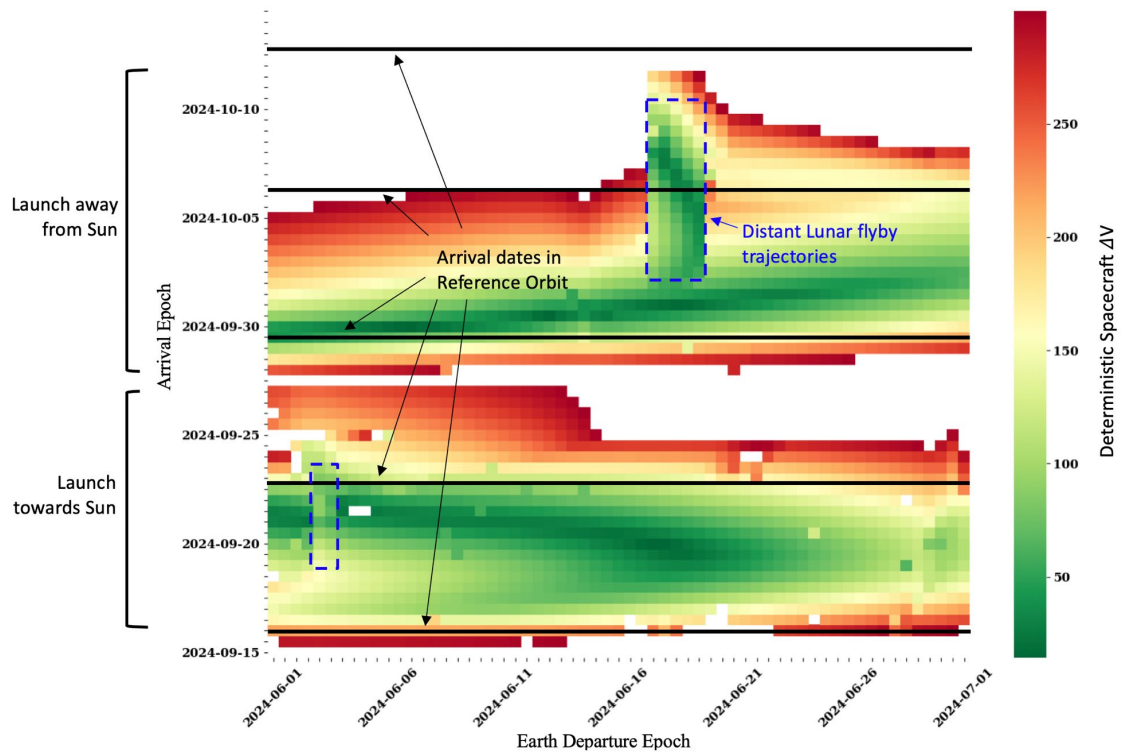


Figure 18. Heatmap of deterministic spacecraft ΔV as a function of Earth departure epoch and NRHO arrival epoch, June 2024.

Finally, the NRHO reference orbit arrival epochs are considered jointly for a 2.5-month period. Figure 19 shows how low ΔV transfers exist for the majority of the sample period. Different families of transfers are selected depending on the Earth departure date. A notional deterministic spacecraft ΔV limit of 60 m/s is drawn in red, with the corresponding launch periods highlighted in green.

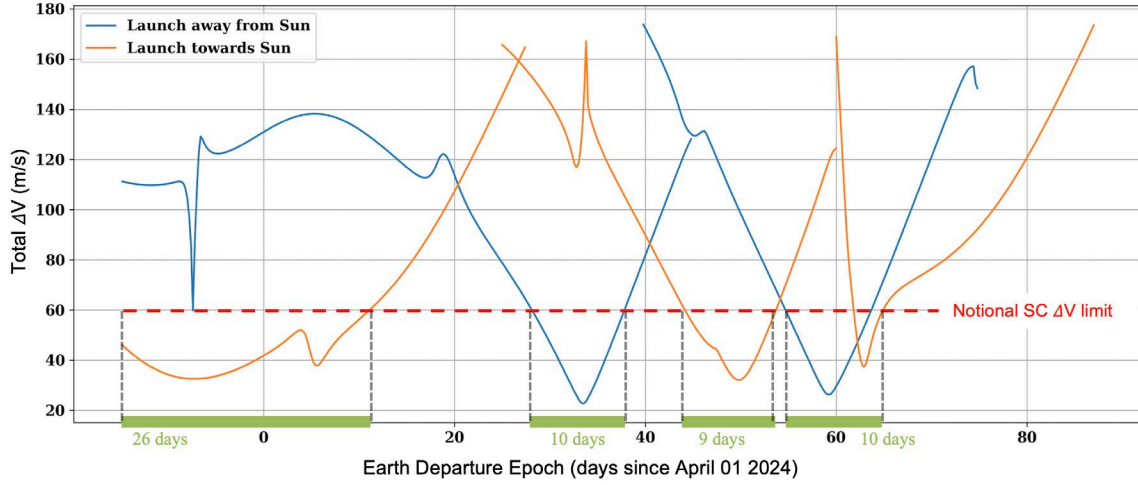


Figure 19. Spacecraft ΔV for multiple months of launch opportunities, phase-fixed with no lunar flyby. Notional launch periods annotated.

Phase-Fixed BLTs with Lunar Flyby

In this section, the phase-fixed (rendezvous) studies are extended to transfers with a lunar flyby shortly after launch. The arrival strategy is assumed to be independent of the rest of the BLT, so the arrival here is the same for all cases: insert-then-rendezvous (ITR) with zero revolutions of wind-on. Recall from the phase-free analysis of lunar flyby transfers that six families of flyby solutions with good performance were identified. Those same families are used here. The goal of the phase-fixed analysis is to understand the launch periods that exist for rendezvous with a reference NRHO.

Each of the six families is evaluated as a point solution every month for one year with optimized departure and arrival epochs, resulting in 78 “seed” solutions. Each of these seed solutions is then used as an initial guess to find other low- ΔV solutions with launch and arrival epochs of approximately ± 1 week. The continuation method is used in two dimensions to initialize solutions at each grid point from nearby good solutions. More than 55,000 of these numerically-sensitive transfers are evaluated in high fidelity. An overview of an entire year (April 2024 – April 2025) is provided in the appendix. Figures 21-23 describe a portion of the analysis over approximately 2 months of launch opportunities. Each figure is a heatmap of an important parameter as a function of Earth departure epoch and NRHO arrival epoch for 6 families of BLTs with an outbound lunar flyby. The dashed horizontal lines represent opportunities to rendezvous with the target NRHO. Figure 20 shows the total deterministic spacecraft ΔV , Figure 21 shows the launch vehicle C3, and Figure 22 shows the altitude of the lunar flyby. Note that it is often possible to trade C3 for ΔV , so variations of these transfers exist. Also note that this analysis, while extensive, is not complete. Gaps are apparent which, in most cases, can be filled in with additional computational effort. Further analysis would add more trajectories to the solution space, so this is a conservative representation.

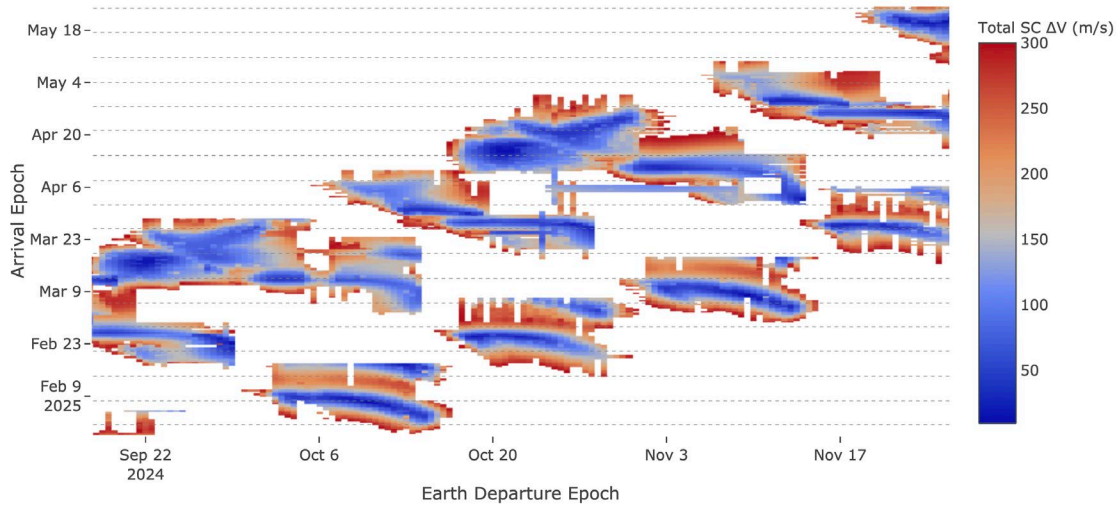


Figure 20. Heatmap of total deterministic spacecraft ΔV for BLTs with lunar flyby.

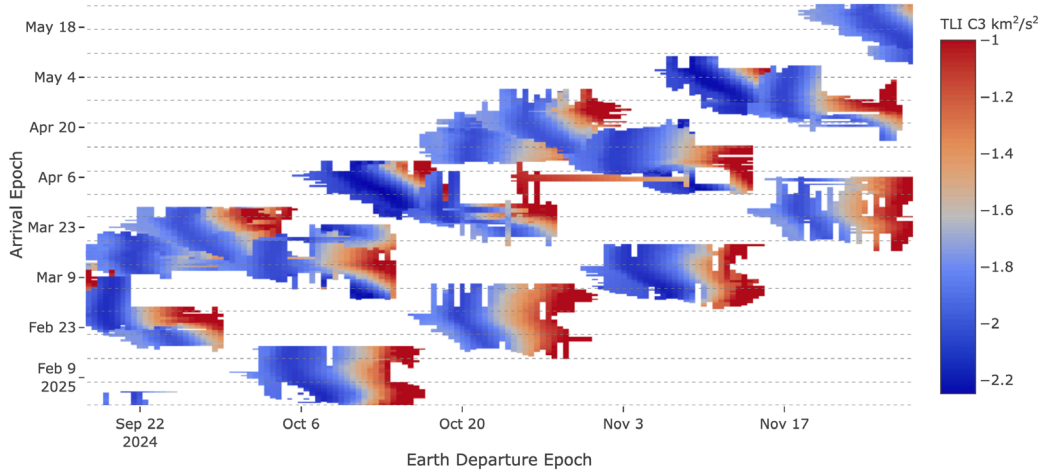


Figure 21. Heatmap of launch vehicle C3 for BLTs with lunar flyby. C3 is limited to ≤ -1.0 km²/s².

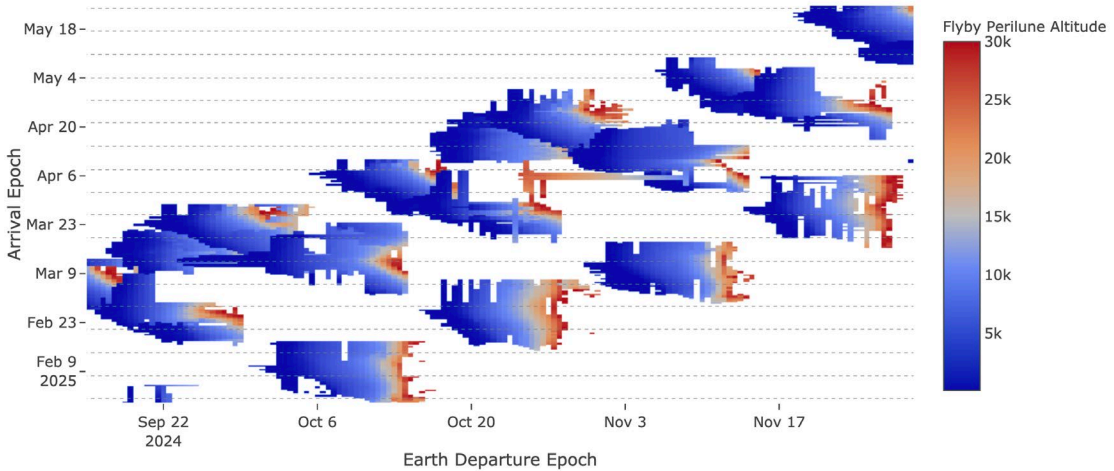


Figure 22. Heatmap of flyby altitude for BLTs with lunar flyby. Altitude constrained to be ≥ 100 km.

From these results, it is possible to describe the launch opportunities for transfers over the course of a full year. Since phase-fixed transfers are required for Gateway elements to rendezvous in the NRHO, the arrival epochs are constrained to the reference orbit perilune epochs (the horizontal dashed lines in the heatmap plots). Figure 23 shows the periods of time over which each of two constraints are met (total deterministic spacecraft $\Delta V \leq 100$ m/s, and $C3 \leq -1.5$ km²/s²) and the periods of time over which solutions are found which satisfy both constraints simultaneously.

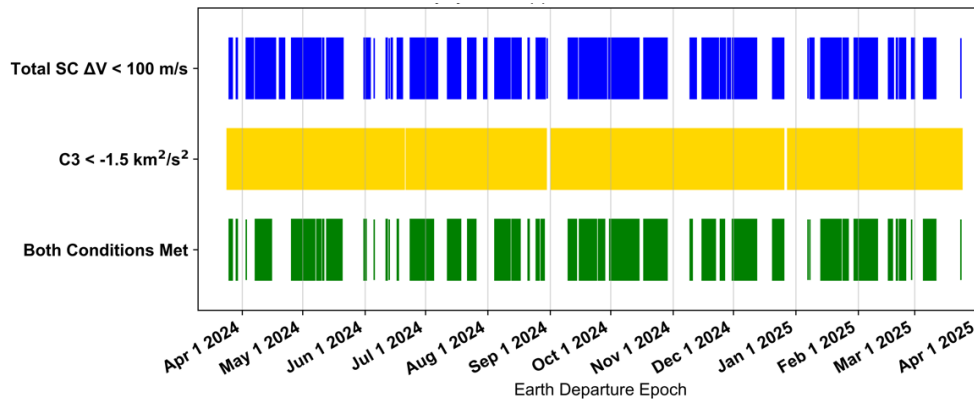


Figure 23. Lunar flyby BLT opportunities to reference NRHO.

These results are then condensed even further. Analysis of the full set of options reveals that there are plentiful launch opportunities that use a BLT with an outbound lunar flyby and rendezvous with a reference NRHO. Between April 1, 2024 and April 1, 2025:

- 66.16% of launch dates have total deterministic spacecraft $\Delta V \leq 100$ m/s,
- 97.81% of launch dates have $C3 \leq -1.5$ km²/s², and
- 56.85% of launch dates meet both conditions.

Additional results are drawn from the same analysis. In the same one-year interval,

- Longest interval where either constraint is not met: 12.5 days
- Longest interval where both constraints are met: 15.5 days
- Average interval where both constraints are met: 4.96 days

Note that additional constraints could reduce the availability of launch options. Some examples of potential additional constraints are: limit maximum eclipse duration, limit time of flight, limit maximum distance from the Earth. Extending the study to additional transfers would counteract this by adding more trajectory options.

CONCLUSION

Using BLTs can reduce the ΔV requirements of a Moon-bound spacecraft by 200-400 meters per second compared to direct transfers. The main trade-offs are increased travel time and increased maximum distance from the Earth. The gravitational attractions of the Earth, Sun, and Moon are used to reduce the energy required from the spacecraft's propulsion system.

Conley first explored the idea of a low-energy transfer to the Moon in 1968,¹⁵ and many authors have considered them since. Many of the larger surveys have been since conducted by co-author Parker¹⁶ and formalized further in Parker and Anderson¹. Various authors since then have carried out limited studies of their applicability to various mission designs¹⁷⁻²⁰. The present work carries out a thorough exploration of BLTs to NRHO, with the goal of tracing out the trade space for future missions. This is particularly relevant for the Gateway, elements of which are currently in development.

A summary of key parameters for BLTs is provided in Table 2. Note that this study is carried out as generally as possible, and all of these parameters are dependent on actual hardware constraints.

Table 2. Typical values of key parameters for BLTs to NRHO.

BLT type	Launch C3 [km ² /s ²]	Deterministic DSM ΔV [m/s]	Deterministic Insertion ΔV [m/s]	Time of flight [weeks]
Without lunar flyby	-0.7 to -0.3	0 to 100	7 to 18	12 to 18
With lunar flyby	-2.2 to -1.5	0 to 100	7 to 18	16 to 25

The present work addresses several important mission design considerations for BLTs. These include description of a diverse set of families of transfers, eclipse analysis, launch period analysis, insertion analysis, and simplified rendezvous analysis. Additional analysis is ongoing to understand insertion and rendezvous in greater depth. Further results will be made available at the Advanced Space website.*

Acknowledgements

The authors wish to thank NASA and the SBIR (Small Business Innovative Research) program for funding this effort.

REFERENCES

1. Parker, J. S. & Anderson, R. L. *Low-Energy Lunar Trajectory Design*. (John Wiley and Sons, 2014).
2. Hill, B. & Creech, S. NASA's Space Launch System: A Revolutionary Capability for Science. (2014).
3. Ocampo, C. A. An Architecture for a Generalized Trajectory Design and Optimization System. in *International Conference on Libration Points and Missions* (2002).
4. Folkner, W. M., Williams, J. G., Boggs, D. H., Park, R. S. & Kuchynka, P. *The Planetary and Lunar Ephemerides DE430 and DE431*. *Interplanet. Netw. Prog. Rep* 196, (2014).
5. Howell, K. C. Three-dimensional, Periodic, 'Halo' Orbits. *Celest. Mech.* 32, 53–71 (1984).
6. Zimovan, E. M., Howell, K. C. & Davis, D. C. Near Rectilinear Halo Orbits and Their Application in Cis-Lunar Space. in *Advances in the Astronautical Sciences* (2017). doi:10.1111/j.1744-6171.2010.00231.x
7. Howell, K. C. & Breakwell, J. V. Almost Rectilinear Halo Orbits. *Celest. Mech.* (1984). doi:10.1007/BF01358402
8. Davis, D. C. *et al.* Orbit Maintenance and Navigation of Human Spacecraft at Cislunar Near Rectilinear Halo Orbits. in *27th AAS/AIAA Space Flight Mechanics Meeting* (2017).
9. Howell, K. C. Families of Orbits in the Vicinity of the Collinear Libration Points. *Journal Astronaut. Sci.* 49, 107–125 (2001).
10. Newman, C. P., Sieling, R., Davis, D. C. & Whitley, R. J. Attitude Control and Orbit Determination of a Crewed Spacecraft With Lunar Lander in Near Rectilinear Halo Orbit. *AAS Astrodyn. Spec. Conf.* 1–19 (2019).
11. Parker, J. S. Families of low-energy lunar halo transfers. *Adv. Astronaut. Sci.* AAS 06-132 (2006).
12. Whitley, R. J. *et al.* Earth-Moon Near Rectilinear Halo and Butterfly Orbits for Lunar Surface Exploration. 1–20
13. Oberth, H. *Ways to Spaceflight*. (R. Oldenbourg Publishing House, 1929).
14. Davis, D. C., Boudad, K. K., Phillips, S. M. & Howell, K. C. Disposal, Deployment, and Debris in

* <https://advancedspace.com/blt/>

- Near Rectilinear Halo Orbits. in *AAS/AIAA Astrodynamics Specialist Conference* (2019).
15. Conley, C. C. Low Energy Transit Orbits in the Restricted Three-Body Problem. *SIAM J. Appl. Math.* 16, (1968).
 16. Parker, J. S. Low-Energy Ballistic Lunar Transfers. (University of Colorado Boulder, 2007).
 17. Topputo, F. Trade-Off Between Cost and Time in Lunar Transfers : a Quantitative Analysis. *24th AAS/AIAA Sp. Flight Mech. Meet. St. Fe, New Mex.* 1–15 (2014).
 18. Folta, D., Woodard, M., Sweetser, T., Broschart, S. B. & Cosgrove, D. Design and Implementation of the ARTEMIS Lunar Transfer Using Multi-Body Dynamics. *Adv. Astronaut. Sci.* 142, 1647–1665 (2012).
 19. Sweetser, T. H. *et al.* ARTEMIS Mission Design. *ARTEMIS Mission* 9781461495, 61–91 (2014).
 20. Folta, D. C., Bosanac, N., Cox, A. & Howell, K. C. The Lunar IceCube Mission Design: Construction of Feasible Transfer Trajectories with a Constrained Departure. in AAS 16-285 (2016).